



# A new experimental and theoretical investigation on the structures of aminoethyl phosphonic acid in aqueous medium based on the vibrational spectra and DFT calculations

María L. Roldán<sup>a</sup>, Ana E. Ledesma<sup>b</sup>, Ana B. Raschi<sup>c</sup>, María V. Castillo<sup>c</sup>, Elida Romano<sup>c</sup>, Silvia A. Brandán<sup>c,\*</sup>

<sup>a</sup> Department of Scientific Research, The Metropolitan Museum of Art, 1000 Fifth Avenue, New York, NY 10028, USA

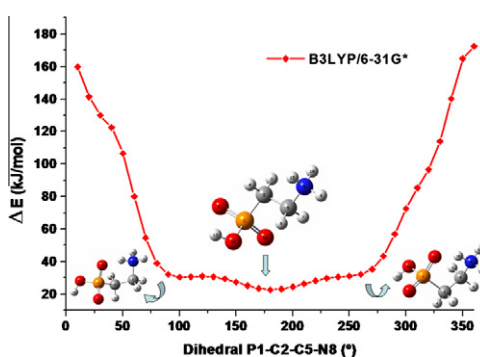
<sup>b</sup> Centro de Investigaciones y Transferencia de Santiago del Estero (CITSE-CONICET), Universidad Nacional de Santiago del Estero, RN 9, km 1125, 4206 Santiago del Estero, Argentina

<sup>c</sup> Cátedra de Química General, Facultad de Bioquímica, Química y Farmacia, Universidad Nacional de Tucumán, Ayacucho 471, 4000 San Miguel de Tucumán, Tucumán, Argentina

## HIGHLIGHTS

- ▶ The zwitterions of the aminoethylphosphonic acid were studied by DFT calculation.
- ▶ A new complete assignment of the observed spectral features is proposed.
- ▶ The solvent effects for the aminoethylphosphonic acid were analyzed using PCM model.
- ▶ The topological properties for the zwitterions in aqueous solution were studied.
- ▶ The charge-transfers for the zwitterions in aqueous solution were investigated.

## GRAPHICAL ABSTRACT



## ARTICLE INFO

### Article history:

Received 19 January 2013

Received in revised form 19 February 2013

Accepted 26 February 2013

Available online 6 March 2013

### Keywords:

Aminoethylphosphonic acid

Vibrational spectra

Molecular structure

Force field

DFT calculations

## ABSTRACT

A new study on the structural and vibrational properties of the aminoethylphosphonic acid was performed in aqueous solution phase by using the self-consistent reaction field (SCRF) method. We have studied and characterized it by infrared and Raman spectroscopies in solid and aqueous solution phases. The Density Functional Theory (DFT) method with Pople's basis set show that three stable zwitterions for the title molecule have been theoretically determined in aqueous solution and that probably they are present in it medium. Here, the solvent effects were studied by means of the self-consistent reaction field (SCRF) method with the polarized continuum model (PCM). The harmonic vibrational frequencies for the optimized geometries of the three zwitterions were calculated at the B3LYP/6-31G\* level of the theory. A complete assignment of the IR and Raman spectra of the compound in aqueous solution was performed combining the DFT calculations with Pulay's Scaled Quantum Mechanics Force Field (SQMFF) methodology in order to fit the theoretical frequency values to the experimental ones. Moreover, Natural Bond Orbital (NBO) and topological properties calculations were performed to analyze the energies and geometrical parameters of its three zwitterions in aqueous medium as well as the magnitude of the intramolecular interactions. The bond orders, atomic charges, solvation energies, dipole moments, molecular electrostatic potentials and force constants parameters calculated for zwitterions in aqueous solution, may be used to gain chemical and vibrational insights into related compounds.

© 2013 Elsevier B.V. All rights reserved.

## 1. Introduction

The organophosphonate compounds are of great chemical and biochemical interest because they have a stable C—P bond highly

\* Corresponding author. Tel.: +54 381 4247752; fax: +54 381 4248169.

E-mail address: [sbrandan@fbqf.unt.edu.ar](mailto:sbrandan@fbqf.unt.edu.ar) (S.A. Brandán).

resistant to chemical hydrolysis, thermal decomposition, and photolysis and, also due to the presence of the phosphate group in their structures they are important macronutrients involved in essential biological processes, such as, the generation of metabolic energy, regulation of cellular signaling pathways, formation of membrane phospholipids, and the structure of nucleic acids [1–18]. On the other hand, the phosphate groups act also as a hydration sensor in lipid bilayers [2,19]. Additionally, the inert nature of C–P bond has effect on the environment when the phosphonates compound, used as a toxic herbicide is accumulating in numerous ecosystems [1,8]. In particular, the aminoethylphosphonic acid (AEP) from their discovery [3–5] is very studied from different points of view [5–16,18]. So, apart from the chemical interest of AEP, the structural and vibrational studies are of mainly biochemical importance because the  $\alpha$ -aminophosphonates compounds have structure analogues to the  $\alpha$ -amino acids and for this reason; they can act as inhibitors of enzymes involved in the metabolism of proteins and aminoacids [6]. Also, AEP has found application in nanotechnology as biofunctionalization agent of iron-oxide nanoparticles for cancer-specific targeting thanks to the formation of strong M–O–P bounds that, unlike other functionalization agents such as silanes, produces monolayers which are highly desirable for preserving the magnetic properties of the nanoparticles [16].

Nowadays, the crystal and molecular zwitterionic structure of AEP in solid phase is well known [9,11] but the structure and properties in aqueous solution, so far, still remain unsolved. The infrared spectrum of AEP in solid phase and the Raman spectra of solid samples obtained from evaporating aqueous solutions at pH 0.5, 4.5 and 13 of the compound were published by Ohno et al. [15]. They have recorded and assigned those spectra in the 1600–100  $\text{cm}^{-1}$  region but the corresponding assignments of the stretching modes related to the  $\text{NH}_3$ ,  $\text{CH}_2$  and  $\text{OH}$  groups in the 4000–2000  $\text{cm}^{-1}$  region were not reported. Additionally, in that work the structural and vibrational analysis of the different zwitterions of AEP in aqueous solution [15] neither the infrared nor Raman spectra of AEP in aqueous solution were published. To the best of our knowledge, there are no theoretical studies concerning geometries and vibrational spectra for the zwitterions of AEP in aqueous solution in the 4000–100  $\text{cm}^{-1}$  region. To identify the zwitterionic species of AEP in all systems by means of vibrational spectroscopy, a complete characterization of those species as well in solid phase as in aqueous solution is very useful. In this context, the aim of this paper is to study, from structural and spectroscopic point of view, the theoretical structures of the more stable zwitterionic forms of AEP in aqueous solution in order to know the structural and vibrational properties of AEP in aqueous medium and, this way, to know the change around of the phosphates groups when AEP is dissolved in water. This study constitutes an important first step toward a detailed understanding of the biological properties of an organophosphonate compound in aqueous medium [20,21]. For that purpose, we optimized the theoretical structures of the zwitterions in aqueous solutions by using the DFT methods and taking into account the solvent effect by means of the SCRF method with the PCM model [22,23]. Afterwards, a complete assignment of all observed bands in the IR and Raman spectra in solid state and in aqueous solution were performed by using an approximate normal coordinate analysis combining DFT calculations with the Pulay's SQMFF methodology [24]. Moreover, to analyze the energies and geometrical parameters of the stable zwitterions of AEP in aqueous solution and the magnitude of the intramolecular interactions, Natural Bond Orbital (NBO) [25,26] and atoms and molecules theory AIM [27,28] calculations were performed. Furthermore, the possible charge-transfer and the intermolecular bond path were analyzed. In addition, two dimeric forms of AEP were also studied in accordance with the

experimental structure determined by means of X-ray diffraction data [9]. Here, the theoretical properties of the studied species are shown and discussed. Good agreement between theoretical and experimental harmonic vibration frequencies was found.

## 2. Experimental methods

A pure MP Biomedicals commercial sample of aminoethylphosphonic acid (AEP) as a crystalline solid was used. The IR spectrum of the solid substance in KBr pellets was recorded in the wavenumbers range from 4000 to 400  $\text{cm}^{-1}$ , while the spectrum of a saturated aqueous solution of the sample between AgCl windows was recorded from 4000 to 400  $\text{cm}^{-1}$  and then the corresponding bands due to the solvent were subtracted. Both studies were performed with a FTIR GX1 Perkin Elmer spectrometer, equipped with a Globar source and DGTS detector. The Raman spectrum of the solid substance was measured in a glass capillary between 4000 and 100  $\text{cm}^{-1}$  while the liquid sample with a saturated solution of AEP in water was conducted with a 10 mm path length glass cuvette. FTIR GX1 Perkin Elmer spectrometer, equipped with Raman accessory was used for all measurements. Raman has a Nd–YAG\* laser (9395  $\text{cm}^{-1}$ ) and an InGaAs detector. All spectra were recorded with a resolution of 1  $\text{cm}^{-1}$  and 200 scans.

## 3. Computational details

The potential energy curves associated with rotation around the C2–C5 bond, described by the P1–C2–C5–N8 dihedral angle for the  $\beta$ -form of AEP is observed in Fig. S1 (Supporting material) at the B3LYP/6-31G\* level of theory [29,30]. The DFT calculations show the presence of three stable zwitterions with geometries  $C_1$ , named zw-1, zw- $\alpha$  and zw- $\beta$  zwitterions, respectively. The zw-1 and zw- $\alpha$  zwitterions have *gauche* conformations with P1–C2–C5–N8 dihedral angles of  $-60$  and  $60^\circ$ , respectively while the zw- $\beta$  zwitterion has a *trans* conformation and a P1–C2–C5–N8 dihedral angle of  $180^\circ$  in accordance with the experimental value [9]. The structures and labeling of the atoms for all zwitterions of AEP in aqueous solution can be seen in Fig. 1. The theoretical structures of the three zwitterions in aqueous solution were computed by using the SCRF method and the solvent effects were simulated considering the cavity of series of spheres using the PCM model, as implemented in the Gaussian 09 program [31]. The solvation energy values were computed by using the solvation model (SMD) which accomplished by performing gas phase and taking the difference in the resulting energies [32]. The NBO calculations were performed by using the NBO 3.1 [26] program, as implemented in the Gaussian 09 package while the electronic charge density topological analysis was performed by using the AIM methodology, by the AIM200 program package [28]. The harmonic wavenumbers and the valence force field expressed in Cartesian coordinates for the zwitterions in aqueous solution were calculated at the same levels of approximation. In both cases, the resulting force fields were transformed to “natural” internal coordinates by using the MOLVIB program [33]. The natural internal coordinates for the zwitterionic species of AEP have been defined as those reported for molecules with similar groups [34–36] and are listed in Table S1 (Supporting material). Following the SQMFF procedure [24], the harmonic force field for the three AEP zwitterions were evaluated at B3LYP/6-31G\* level. The potential energy distribution components (PEDs) higher than or equal to 10% are subsequently calculated with the resulting SQM. The molecular volumes for the zwitterions were calculated by using the MOLDRAW program [37]. The nature of all the vibration modes corresponding to the dimers 1 and 2 of AEP (Figs. S2 and S3, respectively) in aqueous solution at B3LYP/6-31G\* level was carried out

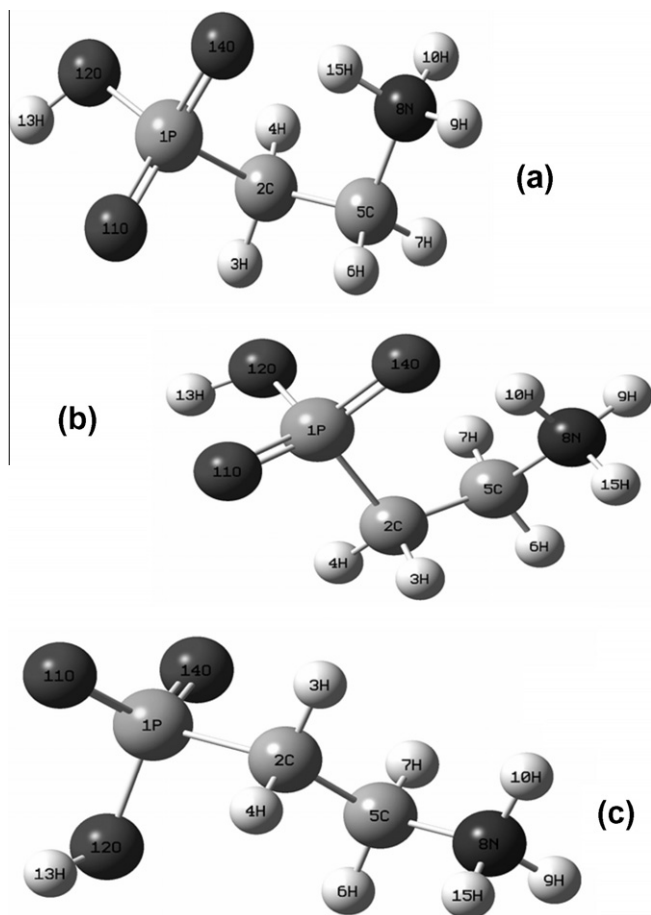


**Fig. 1.** Theoretical structures and atoms numbering for the stable zwitterions of the aminoethylphosphonic acid: (a) zwitterion-1 form, (b) zwitterion- $\alpha$  form, and (c) zwitterion- $\beta$  form.

by means of the *GaussView* program [38]. The total energy for the dimeric species by using the 6-31G\* basis set was corrected for Basis Set Superposition Error (BSSE) by the standard Boys–Bernardi counterpoise method [39].

## 4. Results and discussion

### 4.1. Geometry

A comparison of the total energies and the corresponding dipole moment values for all the stable zwitterionic structures of AEP in aqueous solution by using the B3LYP/6-31G\* method is given in Table S2. The results show that the energies of the zw-1 and zw- $\alpha$  zwitterions are significantly lower than the corresponding to zw- $\beta$ , and that the differences of potential energy between zw-1 and zw- $\alpha$  in reference to zw- $\beta$ , are respectively, 34.88 and 31.73 kJ/mol, respectively. On the other hand, the high value of the dipole moment for zw- $\beta$  could partially explain its stability in aqueous solution, as was observed in other molecules [40–44]. In this study, the zw-1, zw- $\alpha$  and zw- $\beta$  zwitterions of AEP were analyzed in accordance with the experimental *trans* structure reported for the zw- $\beta$  zwitterion [9]. Table 1 show a comparison of the calculated geometrical parameters for those zwitterions by using both methods with the corresponding experimental values obtained [9] by means of the root-mean-square deviation (RMSD) values. The results reveals a good agreement with the experimental bond lengths for the zw-1 and zw- $\beta$  zwitterions while the best

**Table 1**

Comparison of calculated geometrical parameters for the stable zwitterionic forms of the aminoethylphosphonic acid.

Parameter	PCM/B3LYP/6-31G* <sup>a</sup>			Exp <sup>b</sup>
	Zwitterion-1 (gauche)	Zwitterion- $\alpha$ (gauche)	Zwitterion- $\beta$ (trans)	
<i>Bond lengths (Å)</i>				
P1–O11	1.506	1.504	1.516	1.500
P1–O12	1.653	1.657	1.661	1.560
P1–O14	1.534	1.532	1.516	1.510
C2–P1	1.851	1.849	1.839	1.800
C2–C5	1.531	1.530	1.518	1.510
C5–N8	1.509	1.508	1.508	1.480
O12–H13	0.971	0.971	0.973	0.830
N8–H9	1.022	1.022	1.026	0.900
N8–H10	1.023	1.080	1.026	0.900
RMSD	0.028	0.032	0.028	
<i>Bond angles (°)</i>				
C2–C5–N8	109.7	109.8	110.8	111.9
P1–C2–C5	111.8	113.1	112.8	112.0
C2–P1–O12	102.4	102.5	102.4	105.4
O11–P1–O14	120.3	120.9	120.2	115.6
O12–P1–O14	106.1	104.9	105.3	107.7
H9–N8–H10	107.6	111.0	107.8	111.0
P1–O12–H13	109.1	109.8	110.3	114.0
C5–N8–H9	112.2	112.2	111.2	108.0
C5–N8–H10	111.5	105.5	111.0	108.0
RMSD	1.13	1.06	1.00	
<i>Dihedral angle (°)</i>				
P1–C2–C5–N8	–59.3	57.9	–179.8	180.0

<sup>a</sup> This work.

<sup>b</sup> From Ref. [9].

**Table 2**

Molecular volume for the stable zwitterionic forms of the aminoethylphosphonic acid by the B3LYP/6-31G\* method.

Zwitterions	Molar volume (Å <sup>3</sup> )		$\Delta V = V_{AS} - V_G$ (Å <sup>3</sup> ) <sup>a</sup>
	Gas	PCM//SMD	
Zwitterion-1 (gauche)	119.5	119.0	0.5
Zwitterion- $\alpha$ (gauche)	118.2	118.6	0.4
Zwitterion- $\beta$ (trans)	126.7	119.7	–7.0

<sup>a</sup> See text.

results for the bond angles are observed for the zw- $\beta$  zwitterion. It is important to note that the N–H and P–O distances values for all the zwitterions by using PCM model are always larger in solution, compared to the solid phase, due to the solvation. The C2–C5 distance of the zw- $\beta$  zwitterion is practically not affected by hydration. For zw- $\beta$ , the value of the P1–C2–C5–N8 dihedral angle in aqueous medium is of about 180°, as that observed in solid phase while for the zw-1 and zw- $\alpha$  zwitterions those dihedral angles have values of around 60°. Hence, the charge separation is larger in zw- $\beta$  than for the other ones and, for this reason; the dipole moment value in zw- $\beta$  is higher. The differences between the experimental and theoretical results could be attributed to the fact that in solid phase the crystal packing forces are important while in aqueous solution the hydrogen bonding forces prevail, as was also observed in others zwitterions in aqueous solution [34,35]. The calculated molecular volume for the zwitterions, by using the MOLDRW program [37] for the B3LYP/6-31G\* method is observed in Table 2. Zwitterions are species highly hydrated in aqueous solution and consequently; the corresponding volume undergoes an increase or a decrease in this medium, in relation to the values in the gas phase. The volume variations, expressed as a difference between the volume in gas phase and in aqueous solutions by using the PCM/SMD model, show a higher variation (–7.0 Å<sup>3</sup>) for the zw- $\beta$  zwitterion, in agreement with the high uncorrected solvation energy, as can be seen in Table S3.

#### 4.2. Solvation energy

The uncorrected solvation energy ( $\Delta G_u$ ), calculated as relative energy ( $\Delta E$ ) and defined as the difference between the total energies in aqueous solutions and the values in gas phase for the three zwitterions using the 6-31G\* basis set, are presented in Table S3. The uncorrected ( $\Delta G_u$ ) and corrected ( $\Delta G_c$ ) solvation energies together to the total non-electrostatic terms ( $\Delta G_{ne}$ ) due to the cavitation, dispersion and repulsion energies calculated by means the PCM model for all the studied species are given in Table 3. The  $\Delta G_{ne}$  values in aqueous phase were obtained using the PCM/SMD model [32]. The  $\Delta G_c$  values for the three zwitterions of AEP with the two basis sets used increase significantly from zw-1 to zw- $\beta$ , as seen in Table 3. Thus, the higher  $\Delta G_c$  value is obtained for the zw- $\beta$ , due to its larger charge separation, higher value of dipole moment (Table S2) and higher variation of volume in solution (Table 2). These results clearly evidence a higher hydration in aqueous solution for zw- $\beta$ .

#### 4.3. Molecular electrostatic potential, atomic charges, bond orders

The molecular electrostatic potential values for those zwitterions in aqueous solution by using the B3LYP/6-31G\* method are given in Table S4. The most negatives values of molecular electrostatic potential [45–51] were observed for the P atoms and the less negatives for the H atoms belonging to the  $\text{NH}_3^+$  groups for all species in aqueous solution. Note that the energetically lower stability for the zw- $\beta$  zwitterion is justified by the higher molecular electrostatic potential values of the phosphate group that make less stable the molecule. On the other hand, the analysis of the atomic charges derived from the ESPs (MK) [48] using the B3LYP/6-31G\* method, for the three zwitterions are very different from the natural atomic charges, as can be seen in Table S5. We observed that the natural and MK charges values for the O and N atoms are most negative in all zwitterions, while the most positive values are observed for the P and H atoms. Moreover, the different charge values observed on those atoms suggest an unlike formation of H bonds and, thus a different hydration in solution for the three zwitterions is expected. The analysis of the bond orders expressed by Wiberg's indexes for the three AEP zwitterions (Table S6) show that the bond order values for the O and H atoms belonging to the phosphate and  $\text{NH}_3^+$  groups, respectively in the zw- $\beta$  have smaller values than the other ones due to a higher solvation. These results clearly indicate that the hydration in the phosphate and  $\text{NH}_3^+$  groups are different in the three zwitterions and, obviously, the variations in the observed properties are due to the presence of hydrogen bonding that involves those groups.

#### 4.4. NBO analysis

The second order perturbation energies  $E^{(2)}$  (donor  $\rightarrow$  acceptor) that comprise the most important delocalizations for the three

**Table 3**  
Calculated Solvation energies ( $\Delta G$ ) for the stable zwitterions of the aminoethylphosphonic acid.

Species	PCM/B3LYP/6-31G*		
	$\Delta G_u^{\#}$	$\Delta G_{ne}$	$\Delta G_c$
Zwitterion-1 ( <i>gauche</i> )	−101.77	24.70	−77.07
Zwitterion- $\alpha$ ( <i>gauche</i> )	−104.40	24.53	−79.87
Zwitterion- $\beta$ ( <i>trans</i> )	−268.59	26.33	−242.26

$\Delta G_c = \Delta G_{\text{uncorrected}}$ .

$\# \Delta G_{\text{Total non-electrostatic}}$ .

zwitterions of AEP are given in Table S7. These results show principally the following: (i) for the three zwitterions, the principal contributions of the stabilization energies are calculated for the  $\Delta ET_{LP \rightarrow \sigma^*}$  charge transfers corresponding to the lone pairs of the O atoms belonging to the phosphate groups, (ii) the contributions of the stabilization energies for the  $\Delta ET_{\sigma \rightarrow \sigma^*}$  charge transfers are higher for the zw- $\alpha$  and zw- $\beta$  zwitterions, (iii) the contributions of the stabilization energies for the  $\Delta ET_{\sigma^* \rightarrow \sigma^*}$  charge transfers are higher for the zw-1 and zw- $\alpha$  zwitterions, and, (iv) the calculated total stabilization energy favors the zw-1 and zw- $\alpha$  zwitterions indicating its probable presence in aqueous solution.

#### 4.5. AIM analysis

The charge electron density, ( $\rho$ ) and the Laplacian of the electron density,  ${}^2\rho(r)$  for the calculated bond critical Point (BCP) and ring critical points (RCPs) from the topological property analysis for the zw-1 and zw- $\alpha$  zwitterions of AEP are shown in Table S8. The results for both forms in aqueous solution using both basis sets show one BCP and one RCP. The BCPs have the typical properties of the closed-shell interaction and therefore, the values of  $\rho(r)$  are relatively low, the relationship  $|\lambda_1|/\lambda_3$  are  $<1$  and  ${}^2\rho(r)$  are positive indicating that the interaction is dominated by the charge contraction away from the interatomic surface toward each nucleus. A very important result is that neither BCP nor RCP is observed for the zw- $\beta$  form. In the zw-1 and zw- $\alpha$  zwitterions in aqueous solution the O14...H15 and the O14...H10 BCPs, respectively are observed which have the typical properties of the closed-shell interaction [47–49]. The calculations with the other method show for these species the same BCPs but with lower values of ( $\rho$ ) and  ${}^2\rho(r)$ . This analysis clearly shows that the zw-1 and zw- $\alpha$  zwitterions are more stable in aqueous solution.

#### 4.6. Vibrational analysis

The recorded infrared and Raman spectra for the compound in aqueous solution compared with the corresponding in solid phase can be seen respectively in Figs. 2 and 3. For this analysis and in according to the above results, the three zwitterions in aqueous solution were considered. The three AEP zwitterions have 39 normal vibration modes, all active in the infrared and Raman spectra. The experimental and calculated wavenumbers for the 39 expected normal vibration modes by using 6-31G\* basis set together to the corresponding assignment are shown in Table 4. Fig. 4 shows the experimental infrared spectrum of AEP in aqueous solution compared with the corresponding theoretical calculated using B3LYP/

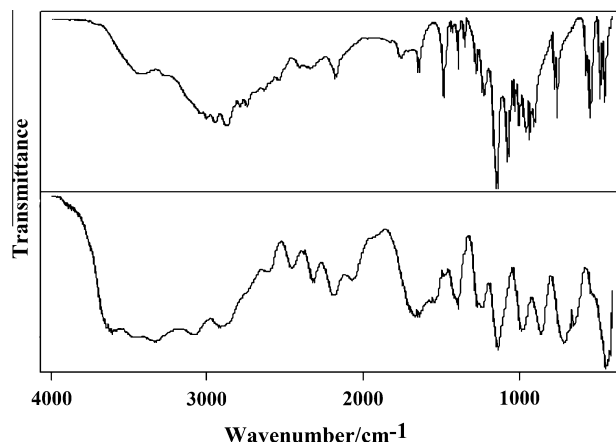


**Fig. 2.** Experimental Infrared spectra of the aminoethylphosphonic acid compound in the 4000–400  $\text{cm}^{-1}$  region: Upper: in solid phase, bottom: in aqueous solution.

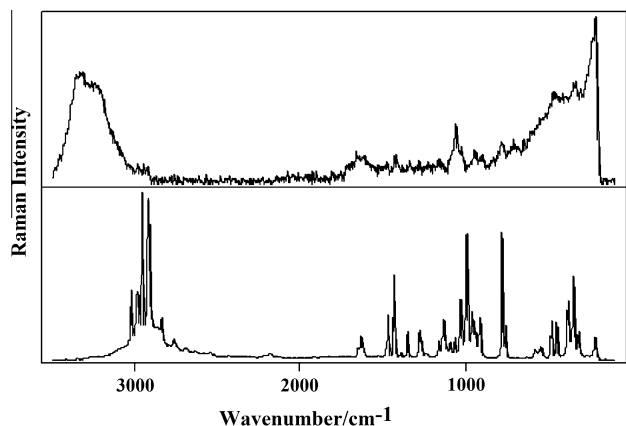


**Fig. 3.** Experimental Raman spectra of the aminoethylphosphonic acid compound in the 4000–100  $\text{cm}^{-1}$  region: Upper: in aqueous solution, bottom: in solid phase.

6-31G\* method for the three zwitterions. The vibrational assignment of the experimental bands to the normal AEP vibration modes is based on the comparison with the previous assignment [15], with related molecules [20,21,34,35,44,45] and with the results of the calculations performed here (Tables S9, S10 and S11). The theoretical infrared spectra for the dimers 1 and 2 of AEP using B3LYP functional and 6-31G\* basis together to the corresponding experimental in aqueous solution can be seen in Fig. S4. Note that the presence of both dimers justifies the occurrence of bands in the 2500–2000  $\text{cm}^{-1}$  region attributed to the H bonds, as is shown in Figs. S2 and S3. The SQM force fields for all the zwitterions of AEP can be obtained at request. The discussion of assignment of the most important groups is presented as follows.

#### 4.6.1. Assignments

**4.6.1.1. OH modes.** As the 4000–2000  $\text{cm}^{-1}$  region is characteristic of the O–H stretching [20,21,34–36,44,45], the broad band in the IR spectrum of the compound in solid phase at 3420  $\text{cm}^{-1}$  and that appears as a strong band at 3610  $\text{cm}^{-1}$  in solution aqueous, is assigned to the O–H stretching. For the dimer 1, the B3LYP/6-31G\* calculations predicted two intense IR bands at 2553 and 2036  $\text{cm}^{-1}$ , which are clearly assigned to the N–H...O–P and P–O...H–N bonds while for the dimer 2 the most intense IR bands at 3347, 3192, and 2061  $\text{cm}^{-1}$  are assigned respectively to the OH...OP, PO–H and N–H...O–P bonds, as is shown in Fig. S4. Taking into account the assignment of L-tyrosine in aqueous solution [34], the IR band and shoulder respectively at 987  $\text{cm}^{-1}$  is assigned to the OH in plane deformation modes for the three zwitterions and the corresponding out-of-plane deformation modes are associated to the Raman bands at 348, 240, and 217  $\text{cm}^{-1}$ . For the  $\text{HPO}_4^{2-}$  ion in aqueous solution, the POH deformation was assigned to the band at 986  $\text{cm}^{-1}$  while the corresponding out-of-plane deformation mode was assigned at 234  $\text{cm}^{-1}$  [21]. These modes were not previously assigned by Ohno et al. [15].

**4.6.1.2. NH<sub>3</sub> modes.** For the three zwitterions of AEP, the theoretical assignments of the three expected N–H stretching modes in aqueous solution for the zw-1 and zw- $\alpha$  zwitterions are different than those for zw- $\beta$ , as observed in Table 4. Thus, for the zw-1 and zw- $\alpha$  zwitterions, the IR bands at 3457 and 3330  $\text{cm}^{-1}$  are assigned to the NH<sub>3</sub> antisymmetric and symmetric stretching modes, respectively, while for zw- $\beta$ , those bands are assigned to the two antisymmetric modes of this group. For zw-1 and zw- $\alpha$ , the remaining antisymmetric modes are calculated at 2373 and 2377  $\text{cm}^{-1}$ , respectively, which can be associated with the weak IR band at 2345  $\text{cm}^{-1}$ . Note that the strong IR and Raman bands

at 3082 and 3240  $\text{cm}^{-1}$ , assigned to the symmetric stretching modes of zw- $\beta$ , support its presence in aqueous solution. These NH<sub>3</sub> stretching modes were not previously assigned by Ohno et al. [15]. According to the calculations, the Raman bands at 1645, 1620, 1475, and 1427  $\text{cm}^{-1}$  are clearly assigned to the antisymmetric and symmetric NH<sub>3</sub> deformation modes corresponding to the three zwitterions. In the previous assignment [15] the symmetric NH<sub>3</sub> deformation mode was not assigned in aqueous solution but it was associated with the band observed at 1558  $\text{cm}^{-1}$  in the spectrum in solid phase. The two rocking modes for the three zwitterions are assigned to the shoulder and bands in the Raman spectrum observed at 1080, 1061, and 992  $\text{cm}^{-1}$ , respectively. Newly, in the previous assignment [15] the rocking mode was not assigned in aqueous solution but instead it was associated with the bands observed at 1134 and 1089  $\text{cm}^{-1}$  in the spectrum in solid phase. As predicted by calculation, the corresponding twisting modes for the zw-1 and zw- $\alpha$  zwitterions were assigned to the Raman band at 307  $\text{cm}^{-1}$  and for zw- $\beta$  in aqueous solution this mode is assigned at 237  $\text{cm}^{-1}$ , as indicated in Table 4. This mode was not previously assigned by Ohno et al. [15].

**4.6.1.3. CH<sub>2</sub> modes.** Here, the theoretical assignments of the four expected C–H stretching modes in aqueous solution for zw-1 and zw- $\alpha$  are different than those for zw- $\beta$ , as was also observed in the above groups. The Raman bands between 3034 and 2942  $\text{cm}^{-1}$  are assigned to the two stretching modes expected for the three zwitterions, as observed in Table 4. The bands at 2921 and 2876  $\text{cm}^{-1}$  are respectively assigned to the C–H symmetric stretching modes of both dimers. These modes were not previously assigned by Ohno et al. [15]. As predicted by the calculation, the Raman and IR bands in the spectra in aqueous solution at 1427 and 1415  $\text{cm}^{-1}$  are easily assigned to the corresponding scissoring modes in agreement to compounds containing these groups [34–36,44,45]. The wagging and rocking modes were assigned by Ohno et al. [15], respectively, between the 1396 and 1312  $\text{cm}^{-1}$  and 896 and 710  $\text{cm}^{-1}$  regions. In this study, the wagging modes are associated with the IR bands in aqueous solution at 1395 and 1271  $\text{cm}^{-1}$  while the expected rocking modes are assigned to the shoulder and band of the medium intensity at 1355 and 1238  $\text{cm}^{-1}$ , respectively, as observed in Table 4. The twisting modes of these groups in the previous assignment were reported at 1342 and 1243  $\text{cm}^{-1}$  [15]. In this work, our SQM calculations for the zw-1, zw- $\alpha$  and zw- $\beta$  zwitterions predict these modes at 748, 743 and 689  $\text{cm}^{-1}$ , respectively. Therefore, they were assigned to the Raman bands at 742 and 707  $\text{cm}^{-1}$ , as indicated in Table 4.

**4.6.1.4. PO<sub>3</sub> groups.** It is important to note in Table 4, that in the previous assignment the tetrahedral PO<sub>3</sub> groups were studied with C<sub>3v</sub> symmetry [15] while in this case they were studied with a local C<sub>2v</sub> symmetry. Therefore, significant differences in the corresponding assignments are expected. Here, the two P=O antisymmetric and symmetric stretching modes are in accordance with the previous assignments [15], and taking into account the calculation results, both modes are assigned to bands appearing on the 1200–1000  $\text{cm}^{-1}$  region. For this reason, the antisymmetric stretching modes for the three zwitterions are associated with the bands at 1222 and 1162  $\text{cm}^{-1}$ , while, the bands at 1026 and 992  $\text{cm}^{-1}$  are easily assigned to the symmetric stretching modes. The P–O stretching for the three zwitterions are clearly assigned, in accordance with calculations and previous assignment [15], to the Raman bands in the spectrum in aqueous solution at 774 and 742  $\text{cm}^{-1}$ . The corresponding wagging, rocking and twisting modes of the phosphate group for the three zwitterions were also assigned as observed in Table 4. These modes were not previously assigned by Ohno et al. [15]. Note that the bands related to the PO<sub>2</sub>

**Table 4**  
Observed and calculated wavenumbers ( $\text{cm}^{-1}$ ), potential energy distribution for the zwitterions of the aminoethylphosphonic acid.

Experimental <sup>b</sup>					Experimental <sup>a</sup>				Zwitterion-1 <sup>a</sup>		Zwitterion- $\alpha$ <sup>a</sup>		Zwitterion- $\beta$ <sup>a</sup>	
Raman Solut pH0.5	Raman Solut pH4.5	Raman Solut pH9	Raman Solut pH13	Assignment	IR solid	Raman Solid	IR Solut	Raman Solut	SQM <sup>c</sup>	Assignment	SQM <sup>c</sup>	Assignment	SQM <sup>c</sup>	Assignment
					3420m		3610s		3594	vO12–H13	3587	v(O12–H13)	3567	v(O12–H13)
							3457s		3387	v <sub>a</sub> NH <sub>3</sub>	3386	v <sub>a</sub> NH <sub>3</sub>	3365	v <sub>a</sub> NH <sub>3</sub>
							3330s	3331vs,br	3317	v <sub>s</sub> NH <sub>3</sub>	3316	v <sub>s</sub> NH <sub>3</sub>	3351	v <sub>a</sub> NH <sub>3</sub>
					3286sh		3082s	3240vs,br					3271	v <sub>s</sub> NH <sub>3</sub>
					3044s	3021m		3034w	3031	v <sub>a</sub> CH <sub>2</sub> (C5)	3033	v <sub>a</sub> CH <sub>2</sub> (C5)	3062	v <sub>a</sub> CH <sub>2</sub> (C5)
					3004s	2988m		2983w	2996	v <sub>s</sub> CH <sub>2</sub> (C2)	2992	v <sub>a</sub> CH <sub>2</sub> (C2)	3004	v <sub>s</sub> CH <sub>2</sub> (C5)
						2979m		2961w	2979	v <sub>s</sub> CH <sub>2</sub> (C5)	2979	v <sub>s</sub> CH <sub>2</sub> (C5)	2980	v <sub>a</sub> CH <sub>2</sub> (C2)
					2956s	2955vs	2949sh	2942w	2940	v <sub>s</sub> CH <sub>2</sub> (C2)	2939	v <sub>s</sub> CH <sub>2</sub> (C2)	2935	v <sub>s</sub> CH <sub>2</sub> (C2)
					2926sh	2916s	2919s	2921w						dim
					2887s	2838w		2888sh						
					2345w	2328vw		2317w	2373	v <sub>a</sub> NH <sub>3</sub>	2377	v <sub>a</sub> NH <sub>3</sub>		
					1643w	1648w	1649s,br	1645w	1603	$\delta$ a NH <sub>3</sub>	1601	$\delta$ a NH <sub>3</sub>	1557	$\delta$ a NH <sub>3</sub>
1628b,w	1629b,w	1630b,w	1650b,w	$\delta$ HOH			1565m	1620w	1576	$\delta$ a NH <sub>3</sub>	1579	$\delta$ a NH <sub>3</sub>	1548	$\delta$ a NH <sub>3</sub>
			1479w	$\delta$ CH <sub>2</sub>	1483m	1476sh	1482w	1475w	1476	$\delta$ s NH <sub>3</sub>	1477	$\delta$ s NH <sub>3</sub>		
			1467w	$\delta$ CH <sub>2</sub>	1467w	1469m			1448	$\delta$ CH <sub>2</sub> (C5)	1447	$\delta$ CH <sub>2</sub> (C5)	1457	$\delta$ CH <sub>2</sub> (C5)
1472w	1470w	1473w	1479w	$\delta$ CH <sub>2</sub>	1432w	1432s		1427w	1425	$\delta$ CH <sub>2</sub> (C2)	1420	$\delta$ CH <sub>2</sub> (C2)	1436	$\delta$ s NH <sub>3</sub>
1424w	1425w	1430w	1479w	$\delta$ CH <sub>2</sub>									1419	$\delta$ CH <sub>2</sub> (C2)
1412sh,vw	1414sh,w	1420sh,w	1418m	$\delta$ CH <sub>2</sub>			1415m		1378	wagCH <sub>2</sub> (C5)	1381	wagCH <sub>2</sub> (C5)	1393	wagCH <sub>2</sub> (C5)
1396vw	1388vw	1384vw	1363vw	wagCH <sub>2</sub> , $\delta$ CH <sub>2</sub>	1390w	1390w	1395m	1382w	1329	$\rho$ CH <sub>2</sub> (C5)	1330	$\rho$ CH <sub>2</sub> (C5)	1351	$\rho$ CH <sub>2</sub> (C5)
1342w	1339w	1338w		$\tau$ CH <sub>2</sub>	1350w	1351w	1355sh	1342w						
			1312w	wagCH <sub>2</sub>										
1272w	1271w	1270w	1279w	POH	1277w	1278w1261w	1271m	1275w	1251	wagCH <sub>2</sub> (C2)	1259	wagCH <sub>2</sub> (C2)	1278	wagCH <sub>2</sub> (C2)
1243vw	1242b,vw	1248sh,vw	1234b,vw	$\tau$ CH <sub>2</sub>		1239vw1230vw	1238m		1234	$\rho$ CH <sub>2</sub> (C2)	1227	$\rho$ CH <sub>2</sub> (C2)	1246	$\rho$ CH <sub>2</sub> (C2)
					1227m	1219vw		1222w			1200	v <sub>a</sub> (PO <sub>2</sub> )		
1175b,m				v <sub>a</sub> (PO <sub>3</sub> )	1156sh	1161w		1162w	1188	v <sub>a</sub> (PO <sub>2</sub> )			1175	v <sub>a</sub> (PO <sub>2</sub> )
	1153b,vw	1148b,vw		v <sub>a</sub> (PO <sub>3</sub> )	1143vs	1132m	1138 s	1140w						
1070sh,w		1078sh,w	1068sh,m	v(C–N)	1074s	1092w		1080sh	1068	$\rho$ NH <sub>3</sub>	1063	$\rho$ NH <sub>3</sub>	1094	$\rho$ NH <sub>3</sub>
1058m	1055vs	1058vw	1051m	v(C–C)	1058w	1064w	1067sh	1061m	1040	$\rho$ NH <sub>3</sub>	1043	$\rho$ NH <sub>3</sub>		
1028m	1025s	1026m		va(POH) <sub>2</sub>	1031w	1029m		1026w					1035	v <sub>s</sub> (PO <sub>2</sub> )
					1002s			992w	1000	v <sub>s</sub> (PO <sub>2</sub> )	1004	v <sub>s</sub> (PO <sub>2</sub> )	1010	$\rho$ NH <sub>3</sub>
		975vs	975vvs	v <sub>s</sub> (PO <sub>3</sub> )		993s	987m,br	970w	975	POH	974	POH	979	POH
954s	952m			vs(POH) <sub>2</sub>	956s	959m	987m,br						975	v(C2–C5)
	934sh,w	938sh,m		v <sub>s</sub> (PO <sub>3</sub> )	933s	938w	940sh	947w	964	v(C2–C5)	961	v(C2–C5)		
896sh,w	907m	905vw		v(C–C), $\rho$ CH <sub>2</sub>	905s	912m		900w	864	v(C5–N8)	864	v(C5–N8)	892	v(C5–N8)
					852sh	854vw	864sh,m,br		840	$\tau$ CH <sub>2</sub> (C5)	847	$\tau$ CH <sub>2</sub> (C5)		
						832vw		786w					838	$\tau$ CH <sub>2</sub> (C5)
	802sh,vw	805w	805sh,vw	$\rho$ CH <sub>2</sub>										
782s	779s	780s	781s	v(C–P),v <sub>s</sub> (PO <sub>3</sub> )	778m	780s	754sh,br	774w	789	v(P1–O12)	778	v(P1–O12)		
745vw	744sh,vw	750sh,vw	750b,vw	$\rho$ CH <sub>2</sub>	757s	758w		742vw	748	$\tau$ CH <sub>2</sub> (C2)	743	$\tau$ CH <sub>2</sub> (C2)	759	v(P1–O12)
710m	710m	711m	710w	v(C–P), $\rho$ CH <sub>2</sub>			713m,br						714	v(C2–P1)
					695sh	683vw		707w					689	$\tau$ CH <sub>2</sub> (C2)
					661vw	664vw	660m	651w	663	v(C2–P1)	657	v(C2–P1)		
	539w	557w	560bw	$\delta$ sPO <sub>3</sub>	572w	573vw		553sh						
				$\tau$ PO, $\delta$ aPO <sub>3</sub>	549s	553vw								
528w				$\delta$ sPO <sub>3</sub>		542w	536w,br	521sh	515	wagPO <sub>2</sub>	520	$\delta$ C5C2P1		
	470m	490m	492m	$\tau$ PO, $\delta$ aPO <sub>3</sub>	484s	480m	479sh	474m					506	$\delta$ PO <sub>2</sub>
455m			455sh,w	$\delta$ aPO <sub>3</sub>	455s	463vw		448m	451	$\delta$ PO <sub>2</sub>				
440sh,m		449w		$\delta$ aPO <sub>3</sub>	448s	448m	443vs,br				437	wag PO <sub>2</sub>		
					433sh	432vw							432	wagPO <sub>2</sub>
					419vw	423vw	420sh	420m	419	$\delta$ v8C5C2	424	$\delta$ PO <sub>2</sub>		
					411sh			395m	392	$\rho$ PO <sub>2</sub>	402	$\delta$ v8C5C2		
						380m		370m					375	$\tau$ PO <sub>2</sub>
334m	344m	349s	347m	$\rho$ PO <sub>3</sub>		348m		332m			328	$\tau$ OH	324	$\rho$ PO <sub>2</sub>

Table 4 (continued)

Experimental <sup>b</sup>			Experimental <sup>a</sup>			Zwitterion-1 <sup>a</sup>		Zwitterion- $\alpha$		Zwitterion- $\beta$		
Raman Solut pH0.5	Raman Solut pH4.5	Raman Solut pH9	Raman Solut pH13	IR solid	Raman Solid	IR Solut	SQM <sup>c</sup>	Assignment	SQM <sup>c</sup>	Assignment	SQM <sup>c</sup>	Assignment
				317w	307m		319	$\tau$ NH <sub>3</sub>	312	$\tau$ NH <sub>3</sub>	304	$\delta$ v8C5C2
				297sh	281sh		296	$\tau$ PO <sub>2</sub>			294	$\delta$ C2P1O12
				288vw	278sh		286	$\delta$ C5C2P1	285	$\delta$ C2P1O12		
				240vw	237m		244	$\tau$ OH	245	$\rho$ PO <sub>2</sub>	254	$\tau$ NH <sub>3</sub>
				227sh	224s		221	$\tau$ PO <sub>2</sub>	221	$\tau$ PO <sub>2</sub>		
				217w	215vs		204	$\delta$ C2P1O12	161	$\tau$ C2-C5	187	$\tau$ OH
				160vw	151vw		159	$\tau$ C2-C5			148	$\delta$ C5C2P1
				138vw	133vw		64	$\tau$ w(PO <sub>2</sub> )	68	$\tau$ w(PO <sub>2</sub> )	88	$\tau$ C2-C5
				106vw	108vw						84	$\tau$ w(PO <sub>2</sub> )

v, stretching;  $\delta$ , scissoring; wag, wagging or out-of-plane deformation;  $\rho$ , rocking;  $\tau$ , torsion, twist, twisting; a, antisymmetric; s, symmetric.

<sup>a</sup> This work.

<sup>b</sup> From Ref [15].

<sup>c</sup> From scaled quantum mechanics force field PCM/B3LYP/6-31G\*.

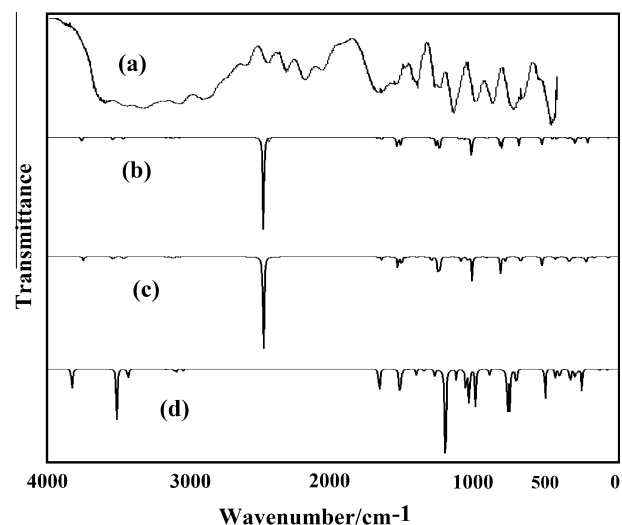


Fig. 4. (a) Experimental infrared spectrum of the aminoethylphosphonic acid compound in aqueous solution compared with the corresponding theoretical calculated using B3LYP functional and 6-31G\* basis set for, (b) zwitterion-1, (c) zwitterion- $\alpha$ , and (d) zwitterion- $\beta$ .

Table 5

Scaled force constants for the stable zwitterionic forms of aminoethylphosphonic acid.

Force constant	PCM/B3LYP/6-31G <sup>a</sup>		
	Zwitterion-1	Zwitterion- $\alpha$	Zwitterion- $\beta$
$f(\nu\text{O-H})$	7.23	7.20	7.12
$f(\nu\text{N-H})$	5.14	5.14	6.16
$f(\nu\text{C-H})$	4.91	4.91	4.90
$f(\nu\text{P=O})$	7.51	7.59	7.61
$f(\nu\text{P-O})$	4.09	4.02	3.81
$f(\nu\text{C-N})$	4.09	4.10	3.87
$f(\nu\text{C-P})$	3.00	3.03	2.87
$f(\nu\text{C-C})$	4.36	4.36	4.26
$f(\delta\text{H-C-H})$	0.84	0.84	0.73
$f(\delta\text{H-N-H})$	0.60	0.60	0.55
$f(\delta\text{P-O-H})$	0.49	0.48	0.49

v, stretching;  $\delta$ , angle deformation.

Units in mdyn  $\text{\AA}^{-1}$  for stretching and mdyn  $\text{\AA} \text{rad}^{-2}$  for angle deformations.

<sup>a</sup> This work.

group change in aqueous solution in relation to the solid phase as consequence of the hydration due to the H bonds.

**4.6.1.5. Skeletal modes.** In the three zwitterions of AEP, the description of the skeletal stretching modes appears strongly mixed among them as can be seen in Tables 4, S9, S10 and S11. The C–N, C–C and C–P stretching modes are predicted by the calculations in different regions for the three zwitterions of AEP. Hence, the Raman band at  $987 \text{ cm}^{-1}$  and the shoulder at  $964 \text{ cm}^{-1}$  are mainly associated with C–C stretching modes while the band in the Raman spectrum in the solid phase at  $912 \text{ cm}^{-1}$ , is associated with the C–N stretching modes of the three zwitterions. The C–P stretching modes are related to the bands at  $713$  and  $660 \text{ cm}^{-1}$ . Finally, the observed modes in the lower wavenumber region ( $330\text{--}100 \text{ cm}^{-1}$ ) for the three zwitterions of AEP were not characterized by Ohno et al. [15]. In this work, those modes are identified and assigned, as observed in Table 4.

#### 4.7. Force field

The force constants expressed in terms of simple valence internal coordinates were calculated from the corresponding

scaled force fields by using the MOLVIB program [33]. A comparison of the principal force constants for the three zwitterions of AEP calculated in aqueous solution is given in Table 5. Note that the values for  $zw-1$  and  $zw-\alpha$  are practically similar between them while slightly change for  $zw-\beta$ . In general, the  $f(O-H)$ ,  $f(C-H)$  and  $f(vN-H)$  values are in agreement with those reported for molecules with similar groups [34–36,44,45]. Here, the  $f(O-H)$  force constants have values between 7.12 and 7.49 mdyne  $\text{\AA}^{-1}$ , as the reported for chloro-quinolin-8-yloxy acetic acid compounds [44] and, greater values compared with the two zwitterions most stable of tyrosine in aqueous solution [34]. Obviously, the observed variations between both compounds are justified by the different involved groups, which are the P–OH group in AEP and the C–OH group in tyrosine. Previously [15], the force constants for the  $NH_3^+-CH_2C$  and  $CCH_2PO_3-H^-$  moieties of AEP were transferred from those for glycyltaurine [52] and aminomethylphosphonic acid [53], respectively. Thus, the C–N, C–C and C–P force constants values were assumed as those for taurine [54], with a value for the C–P stretching force constant of 3.6 mdyne  $\text{\AA}^{-1}$ , in slightly agreement with the values reported here for AEP. Finally, the different force constants of AEP in aqueous solution are attributed to the unlike hydration of the involved groups in each zwitterion. The lower values of the  $f(vO-H)$  and  $f(vP-O)$  force constants for the  $zw-\beta$  zwitterion are in accordance with the H bonds formed due to its higher hydration.

## 5. Conclusions

We have characterized the substance by infrared and Raman spectroscopic techniques in aqueous solution. The theoretical molecular structures of the three zwitterions and the two dimeric forms derived from the aminoethylphosphonic acid were determined in aqueous solution by using the B3LYP/6-31G\* method employing the PCM model. The stability of the three zwitterions was justified by means of the bond orders, atomic charges, solvation energies, dipole moments, molecular electrostatic potentials, intramolecular delocalization energies and AIM analysis. The calculated harmonic vibrational frequencies for the aminoethylphosphonic acid are consistent with the observed infrared and Raman spectra in aqueous solution. The presence of bands attributed to the zwitterions  $zw-1$ ,  $zw-\alpha$  and  $zw-\beta$  and the two dimeric forms of the aminoethylphosphonic acid was detected in the IR and Raman spectra in aqueous solution phase and a complete assignment of the vibrational modes was accomplished. The previously reported assignments [15] were confirmed, corrected and completed in accordance with the present theoretical results. The SQM force fields for all the zwitterions of the aminoethylphosphonic acid were obtained after adjusting the theoretical force constants to minimize the mean deviation between observed and calculated frequencies. Differences in the studied properties for the three zwitterions were found, especially for the  $zw-\beta$  zwitterion, which are justified by the presence of the hydrogen bonding between phosphate and amino groups which appears to have influence on the solvation energies. A higher solvation energy calculated for the  $zw-\beta$  zwitterion reveals its presence in aqueous solution and suggest a higher hydration of this zwitterion. The PCM model used in this study highlights the relevance of the solvent effects. The variations observed on the solvation energies are principally related to the hydrogen bonding and the donor–acceptor interactions.

## Acknowledgements

This work was founded with grants from CIUNT (Consejo de Investigaciones, Universidad Nacional de Tucumán). The authors thank Prof. Tom Sundius for his permission to use MOLVIB.

## Appendix A. Supplementary material

Supplementary data associated with this article can be found, in the online version, at <http://dx.doi.org/10.1016/j.molstruc.2013.02.032>.

## References

- [1] M.A. Adams, Y. Luo, B. Hove-Jensen, S.-M. He, L.M. van Staaldnuin, D.L. Zechel, Z. Jia, *J. Bacteriol.* 190 (3) (2008) 1072.
- [2] V. Luzzati, F.J. Husson, *J. Cell Biol.* 12m (1962) 207.
- [3] M. Horiguchi, M. Kandatsu, *Bull. Agr. Chem. Soc. Jpn.* 24 (1960) 565.
- [4] M. Horiguchi, M. Kandatsu, *Agr. Biol. Chem. Jpn.* 26 (1962) 721.
- [5] M. Horiguchi, M. Kandatsu, *Agr. Biol. Chem. Jpn.* 28 (1964) 408.
- [6] A.-M. Lacoste, M. Poulsen, A. Cassaigne, E. Neuzil, *Curr. Microbiol.* 2 (1979) 113.
- [7] A.S. Paraskar, A. Sudalai, *ARKIVOC* 2006 (x) 183.
- [8] N.G. Ternan, J.W. McGrath, G. McMullan, J.P. Quinn, *J. Microbiol.* 14 (1998) 635.
- [9] Y. Okaya, *Acta Cryst.* 20 (1966) 712–715.
- [10] J.S. Kitredage, E. Roberts, N.G. Simonsen, *Biochemistry* 1 (1962) 624.
- [11] P.M. Darriet, J. Darriet, A. Cassaigne, E. Neuzil, *Acta Cryst.* 20 (1975) 469.
- [12] J.F. Villarreal-Chiu, J.P. Quinn, J.W. McGrath, *Front. Microb.* 3 (2012) 1.
- [13] X. Ma, X. Fu, L. Li, J. Chen, *Molecules* 6 (2001) 390.
- [14] E.D. Naydenova, P.T. Todorov, K.D. Troev, *Amino Acids* 38 (2010) 23.
- [15] K. Ohno, Y. Mandai, H. Matsuura, *J. Mol. Struct.* 298 (1993) 1.
- [16] M. Das, D. Mishra, T.K. Maiti, A. Basak, P. Pramanik, *Nanotechnology* 19 (2008) 415101.
- [17] A. Cuisset, G. Mouret, O. Pirali, P. Roy, F. Cazier, H. Nouali, J. Demaison, *J. Phys. Chem. B* 112 (39) (2008) 1251.
- [18] B. Vilanova, J.M. Gallardo, *J. Phys. Chem. A* 116 (2012) 1897.
- [19] E.A. Disalvo, F. Lairon, S. Diaz, J. Arroyo, *Research Signpost*, 37/66, vol. 2, 2002 (Trivandrum, Kerala, India).
- [20] S.A. Brandán, S.B. Díaz, J.J. López González, E.A. Disalvo, A. Ben Altabef, *Spectrochim. Acta Part A* 66 (2007) 884.
- [21] S.A. Brandán, S.B. Díaz, R. Cobos Picot, E.A. Disalvo, A. Ben Altabef, *Spectrochim. Acta Part A* 66 (2007) 1152.
- [22] J. Tomasi, M. Persico, *Chem. Rev.* 94 (1994) 2027.
- [23] S. Miertus, E. Scrocco, J. Tomasi, *Chem. Phys.* 55 (1998) 1117.
- [24] P. Pulay, G. Fogarasi, F. Pang, E. Boggs, *J. Am. Chem. Soc.* 101 (10) (1979) 2550.
- [25] A.E. Reed, L.A. Curtis, F. Weinhold, *Chem. Rev.* 88 (6) (1988) 899.
- [26] E.D. Glendenning, J.K. Badenhop, A.D. Reed, J.E. Carpenter, F. Weinhold, *NBO 3.1*, Theoretical Chemistry Institute, University of Wisconsin, Madison, WI, 1996.
- [27] R.F.W. Bader, *Atoms in Molecules, A Quantum Theory*, Oxford University Press, Oxford, ISBN: 0198558651, 1990.
- [28] F. Biegler-König, J. Schönbohm, D. Bayles, *J. Comput. Chem.* 22 (2001) 545.
- [29] A.D. Becke, *Phys. Rev. A* 38 (1988) 3098.
- [30] C. Lee, W. Yang, R.G. Parr, *Phys. Rev. B* 41 (1988) 785.
- [31] M.J. Frisch, G.W. Trucks, H.B. Schlegel, G.E. Scuseria, M.A. Robb, J.R. Cheeseman, J.A. Montgomery Jr., T. Vreven, K.N. Kudin, J.C. Burant, J.M. Millam, S.S. Iyengar, J. Tomasi, V. Barone, B. Mennucci, M. Cossi, G. Scalmani, N. Rega, G.A. Petersson, H. Nakatsuji, M. Hada, M. Ehara, K. Toyota, R. Fukuda, J. Hasegawa, M. Ishida, T. Nakajima, Y. Honda, O. Kitao, H. Nakai, M. Klene, X. Li, J.E. Knox, H.P. Hratchian, J.B. Cross, C. Adamo, J. Jaramillo, R. Gomperts, R.E. Stratmann, O. Yazyev, A.J. Austin, R. Cammi, C. Pomelli, J. W. Ochterski, P.Y. Ayala, K. Morokuma, G.A. Voth, P. Salvador, J.J. Dannenberg, V.G. Zakrzewski, S. Dapprich, A.D. Daniels, M.C. Strain, O. Farkas, D.K. Malick, A.D. Rabuck, K. Raghavachari, J.B. Foresman, J.V. Ortiz, Q. Cui, A.G. Baboul, S. Clifford, J. Cioslowski, B.B. Stefanov, G. Liu, A. Liashenko, P. Piskorz, I. Komaromi, R.L. Martin, D.J. Fox, T. Keith, M.A. Al-Laham, C.Y. Peng, A. Nanayakkara, M. Challacombe, P.M.W. Gill, B. Johnson, W. Chen, M.W. Wong, C. Gonzalez, J.A. Pople, *Gaussian 09, Revision A.02*, Gaussian, Inc.: Pittsburgh, PA, 2009.
- [32] A.V. Marenich, C.J. Cramer, D.G. Truhlar, *J. Phys. Chem. B* 113 (2009) 6378–6396.
- [33] T. Sundius, *J. Mol. Struct.* 218 (1990) 321–326.
- [34] C.D. Contreras, A.E. Ledesma, H.E. Lanús, J. Zinczuk, S.A. Brandán, *Vib. Spectrosc.* 57 (2011) 108–115.
- [35] P. Leyton, J. Brunet, V. Silva, C. Paipa, M.V. Castillo, S.A. Brandán, *Spectrochim. Acta Part A* 88 (2012) 162–170.
- [36] P. Leyton, C. Paipa, A. Berrios, A. Zárate, S. Fuentes, M.V. Castillo, S.A. Brandán, *J. Mol. Struct.* 1031 (2013) 110–118.
- [37] P. Ugliengo, *MOLDRAW Program*, University of Torino, Dipartimento Chimica IFM, Torino, Italy, 1988.
- [38] A.B. Nielsen, A.J. Holder, *Gauss View 5.0, User's Reference*, GAUSSIAN Inc., Pittsburgh, PA, 2000–2008.
- [39] S.F. Boys, F. Bernardi, *Mol. Phys.* 19 (1973) 553.
- [40] A.E. Ledesma, S.A. Brandán, J. Zinczuk, O.E. Piro, J. López González, A. Ben Altabef, *J. Phys. Org. Chem.* 21 (12) (2008) 1086–1097.
- [41] S.A. Brandán, G. Benzal, J.V. García-Ramos, J.C. Otero, A. Ben Altabef, *Vib. Spect.* 46 (2008) 89–99.
- [42] J.R. Sambrano, A.R. de Souza, J.J. Queralto, M. Oliva, J. Andrés, *Chem. Phys.* 264 (2001) 333–340.
- [43] S.A. Brandán, *J. Mol. Struct.* 993 (2011) 225–231.
- [44] E. Romano, M.V. Castillo, J.L. Pergomet, J. Zinczuk, S.A. Brandán, *J. Mol. Struct.* 1018 (2012) 149–155.



- [45] L.C. Bichara, H.E. Lanús, C.G. Nieto, S.A. Brandán, J. Phys. Chem. A 114 (2010) 4997–5004.
- [46] A.E. Ledesma, J. Zinczuk, J.J. López González, A. Ben Altabef, S.A. Brandán, J. Raman Spectrosc. 41 (2010) 587–597.
- [47] A.E. Ledesma, J. Zinczuk, J.J. López González, A. Ben Altabef, S.A. Brandán, J. Mol. Struct. 322 (2009) 924–926.
- [48] B.H. Besler, K.M. Merz Jr., P.A. Kollman, J. Comput. Chem. 11 (1990) 431–439.
- [49] S.A. Brandán, J. Mol. Struct. (THEOCHEM) 908 (2009) 19–25.
- [50] A.E. Ledesma, C. Contreras, J. Svoboda, A. Vektariane, S.A. Brandán, J. Mol. Struct. 967 (2010) 159–165.
- [51] J. Zinczuk, A.E. Ledesma, S.A. Brandán, O.E. Piro, J.J. López-González, A. Ben Altabef, J. Phys. Org. Chem. 22 (2009) 1166–1177.
- [52] C. Garrigou-Lagrange, H. Jensen, M. Cotrait, J. Mol. Struct. 36 (1977) 275.
- [53] C. Garrigou-Lagrange, C. Destrade, C.R. Acad. Sci. Ser. C 280 (1975) 969.
- [54] K. Ohno, Y. Mandai, H. Matsuura, J. Mol. Struct. 268 (1992) 41.